doi.org/10.36721/PJPS. 2023.36.2.REG.535-540.1

Formulation and evaluation of chitosan-based nanogel for oral delivery of diosmin

Mohammed Ali Mujtaba[1]* and Nawaf M Alotaibi[2]
[1]Department of Pharmaceutics, Faculty of Pharmacy, Northern Border University, Rafha Campus, Saudi Arabia
[2]Department of Clinical Pharmacy, Faculty of Pharmacy, Northern Border University, Rafha Campus, Saudi Arabia

Abstract: The bioactive flavonoid diosmin (DSN) has a variety of biological activities, excellent therapeutic activity, however, it has a number of biopharmaceutical problems that limit its advantages. The present study aims to develop chitosan-based nanogels (NGs) as drug-delivery platforms for DSN and characterize them using physicochemical methods. DSN-loaded NGs were prepared using the ionic gelation method and particle size (PS), poly-dispersity index (PDI), zeta potential (ZP), loading efficiency (LE), and loading capacity (LC) of 113.07±12.62nm, 0.266±0.08, 22.32± 0.56 mV, 81.56±2.65% and 10.25±1.43% were obtained, respectively. Transmission electron microscopy analysis of DSN-loaded NGs also revealed that the PS ranged from 100 to 200nm, which is comparable to the outcomes of the dynamic light scattering technique. The NGs swelled in pH 6.8 and pH 7.4 buffers and was easily eroded at pH 1.2 and pH 4.5. DSN was released from NGs in acidic buffers by a Fickian process and this release was followed by both swelling and erosion. According to stability experiments, the PS, ZP and PDI at 25ºC and 40ºC did not significantly change after 90 days. In conclusion, the NGs system proved very effective at delivering DSN orally.

Keywords: Diosmin; nanogels; chitosan; particle size; drug release

INTRODUCTION

Most plants and fruits, especially those from the Citrus spp., contain the poorly soluble flavone diosmin (3,5,7-trihydroxy-4-methoxyflavone 7-rutinoside), which has excellent therapeutic potentials in addition to a reported safety profile and excellent tolerance (Caristi *et al*., 2003). Diosmin (DSN) has been used to treat venous leg ulcers and hemorrhoids as a vascular protector for more than 30 years due to its phlebotonic characteristics (El-Shafae and El-Domiaty, 2001). DSN exhibits high antioxidant properties (Kandaswami and Middleton, 1994), in addition to other promising potential effects such as anti-inflammatory (Di Perri and Auteri, 1988), anti-cancer (Dung *et al*., 2012) and anti-ulcer (Izzo *et al*., 1994) properties. Additionally, a lot of studies have looked into DSN as an adjunct to chemotherapy treatment for colon, hepatocellular and urinary bladder carcinogenesis due to its advantages of lower costs and fewer side effects (Dung *et al*., 2012). Additionally, DSN has shown anti-inflammatory properties (Lonchampt *et al*., 1989) and anti-hyperglycemic actions (Pari and Srinivasan *et al*., 2010). Although DSN has a wide range of medicinal applications, their phenolic composition makes them polar yet poorly water soluble and scanty absorption has been reported as a result (Havsteen, 2002). These characteristics act as a barrier to the widespread acceptance of DSN in the pharmaceutical industry. The low bioavailability and substantial inter-subject variability of the medication after oral administration are caused by inadequate drug dissolution (Serra *et al*., 2008).

When compared to other prescribed methods, oral delivery offers several benefits, such as the convenience of use, ease of dose modification, low cost and others, making it the most practical route for providing medications. The ability of nanogels (NGs) to prolong the period that pharmaceuticals remain in the gastrointestinal tract, desired medication release in the GI tract, prevent them deteriorating in the GI fluid and subsequently increased drug absorption across GI membranes which makes them a potential oral drug delivery system. NGs are nanoscale networks of physically or chemically interconnected polymers that are capable of encapsulating medicines by modes of self-assembly including Van der Waals, electrostatic and hydrophobic interactions between the polymer and drug moieties (Kabanov and Vinogradov, 2008). It displays many benefits that are present in both nanoscale carriers and hydrogels. For instance, NGs are simple to administer and have a three-dimensional structure that can swell 1-30 times, from which medications are predicted to have a prolonged release (Moya-Ortega *et al*., 2012). Additionally, due to their nanoscale size, NGs can result in a large specific surface area, which will subsequently boost the solubility and pharmacokinetics of the coupled pharmaceutical molecules (Pérez *et al*., 2014). As a result, NGs have a lot of potential for use in drug delivery systems since they can control drug release and pharmacokinetic characteristics.

Chitosan (CH) has been extensively researched as a nanoscopic drug delivery system due to its interesting properties, including biocompatibility, biodegradability, antibacterial properties, nontoxicity and low cost (Sharma

**Corresponding author:* e-mail: sajanqa@gmail.com

et al., 2018; Kurdtabar *et al*., 2018). Along with these benefits, the presence of main amino (NH_2) and hydroxyl (OH) groups in the CH chain promotes its surface engineering chemical processes (Yu *et al*., 2017). NGs based on CH have attracted a lot of attention recently since they can encapsulate a variety of medications, including proteins, peptides and small molecules etc., to reduce burst release, control release rate, increase efficiency, and enhance the selectivity of the therapy. Therefore, in this study, chitosan-based DSN-loaded NGs were prepared using an ionic gelation technique, and their swelling, morphology, and swelling properties were assessed. Additionally, *in vitro* drug release in various buffers is also evaluated. The current study will yield some useful outcomes for efficiently delivering DSN and enhancing the route of administration of NGs.

MATERIALS AND METHODS

Materials

Chitosan with a medium molecular weight and a deacetylation level of 85% was bought from Sigma-Aldrich, St. Louis, Missouri, USA. Diosmin was received from Jamjoom Pharmaceutical Co. Ltd. (Jeddah, Saudi Arabia) as a gift sample. Sodium tripolyphosphate (TPP) was bought from CDH Labs in India and other chemicals utilized were of analytical grade.

Preparation of DSN-loaded chitosan nanogels (DSN-NGs) formulation

The NGs were formed by ionizing CH with a polyanion called TPP. A clear solution (CH, 2.5mg/mL) was created in the technique by dissolving the CH polymer in a 2%v/v acetic acid solution while stirring. The mixture was then constantly stirred overnight. TPP (2.5mg/mL) and DSN (1 mg/mL) solutions in water were also made in parallel. Following that, a dropwise addition of the anionic TPP/DSN solution was made to the cationic CH solution (1:2 volume ratio), with a steady flow rate and continued stirring for 60 minutes. To produce DSN-loaded nanogels, the resultant solution was probe-sonicated (SONICS Vibra cell VC750, USA) with a 30% amplitude in pulsed mode for 10 minutes in an ice bath.

Characterization of DSN-NGs formulation

Particle size, zeta potential and polydispersity index

A dynamic light scattering (DLS) (Malvern Zetasizer, Nano ZS, UK) method was used to calculate the particle size (PS), polydispersity index (PDI) and zeta potential (ZP) of the DSN-NGs formulation. To prevent the multi-scattering phenomenon, samples were appropriately diluted with distilled water before the measurement. The temperature was held constant at about 25±2ºC while the scattering angle was kept at 90º. A triplicate of each measurement was made (Mujtaba *et al*., 2022).

Loading efficiency and loading capacity

To assess the loading efficiency (LE) and loading capacity (LC) of DSN in NGs, NGs dispersions were first centrifuged (15,000g for 10min). The supernatants were then collected and the free DSN was analyzed using spectrophotometrically (UV-1100, Shimadzu Ltd., Japan) at 269 nm (Abd El Hady *et al*., 2019). Equations 1 and 2 were used, respectively, to calculate the LE and LC:

$$\text{Loading Efficiency (LE)} = \frac{\text{Amount of drug added in NG} - \text{free drug in the supernatant}}{\text{Amount of drug added in NG}} \times 100 \quad (1)$$

$$\text{Loading Capacity (LC)} = \frac{\text{Amount of drug added in NG} - \text{free drug in the supernatant}}{\text{Total weight of NG}} \times 100 \quad (2)$$

Determination of swelling ratios (SR)

A small amount of freeze-dried gel (0.2g) was dissolved at a temperature of 37°C in 5mL of phosphate buffer having pH 6.8 and pH 7.4. The swelled gels were weighed after the extra water on their surfaces was carefully removed using filter papers at regular intervals. The SR of the gels was calculated using equation 3 at each time point.

$$SR = \frac{\text{Weight of swollen sample} - \text{weight of dry sample}}{\text{weight of dry sample}} \quad (3)$$

Morphological analysis using transmission electron microscopy (TEM)

TEM was used to characterize the morphology and potential aggregation of the NGs. The samples were then appropriately diluted with water and placed a drop of the samples on a copper grid that had been coated with carbon, the grid was dried and 1% phosphotungstic acid was used to negatively stain it. For TEM (Zeiss, model EM10C, Germany) observations, the dried coated grid was set over the slide and covered with a coverslip (Soni *et al*., 2020).

In vitro drug release and kinetic studies

When formulations are taken orally, they move through various gastrointestinal tracts and are subjected to various pH conditions. Accordingly, in different pH media, the in vitro release of DSN from NGs was assessed. The *in vitro* release characteristics of DSN from the formulation of DSN-NGs were investigated accordingly to the reported method (Yao *et al*., 2016). 1mL of NGs and an equal volume of medium ware sealed inside a dialysis bag, and the bag will be shaken horizontally at 120 revolutions per minute while dialyzing against 35 milliliters of different buffers (pH1.2 HCl, pH4.5 acetate and pH6.8 phosphate). 1mL of the medium was removed and immediately replaced with an equivalent amount of fresh media at specified intervals. A double beam UV/Visible spectrophotometer was used to measure the amount of DSN in the release medium at λ max of 269 nm (Abd El Hady *et al*., 2019). All drug release tests were performed three times.

To better understand the drug release phenomena from the formulation of DSN-NG, the *in vitro* drug release data were fitted to a number of release kinetics models, including zero order, first order, Higuchi model and Korsmeyer-Peppas model.

Table 1: Nanogels characterization

Formulation	Mean particle size (nm)	Zeta potential (mV)	LE (%)	LC (%)
DSN-loaded NGs	113.07 ± 12.62	22.32 ± 0.56	81.56 ± 2.65	10.25 ± 1.43

Table 2: Drug release kinetic data of DSN-NGs formulation[a]

Model	Equation	R^2 Value		
		pH 1.2 (0-12h)	pH 4.5 (0-12h)	pH 6.8 (0-12h)
Zero order	mo - m = kt	0.8632	0.8748	0.7214
First order	ln m = kt	0.9863	0.9715	0.7322
Higuchi's model	mo - m = $kt^{1/2}$	0.9764	0.9781	0.8531
Korsmeyer–Peppas	log (mo - m) = log K + n log t	0.9759	0.9751	0.6776

[a] m_o is the initial drug amount (100%); m the amount of drug remaining at a specific time; k is the rate constant; t is the time.

Table 3: Stability data

DSN-NGs formulation (25°C ± 2°C)				
Parameters	0 days	30 days	60 days	90 days
Particle size (nm)	113.07 ± 12.62	120.21 ± 10.53	133.2 ± 14.23	132.6 ± 15.83
PDI	0.266 ± 0.08	0.291 ± 0.07	0.296 ± 0.10	0.298 ± 0.12
Zeta potential (mV)	22.32 ± 0.56	23.62 ± 1.11	22.71 ± 1.13	23.54 ± 1.21
DSN-NGs formulation (40°C ± 2°C)				
Parameters	0 days	30 days	60 days	90 days
Particle size (nm)	113.07 ± 12.62	124.33 ± 11.13	141.6 ± 13.63	139.8 ± 14.26
PDI	0.266 ± 0.08	0.298 ± 0.11	0.302 ± 0.10	0.311 ± 0.13
Zeta potential (mV)	22.32 ± 0.56	22.85 ± 1.01	23.01 ± 1.08	23.33 ± 1.11

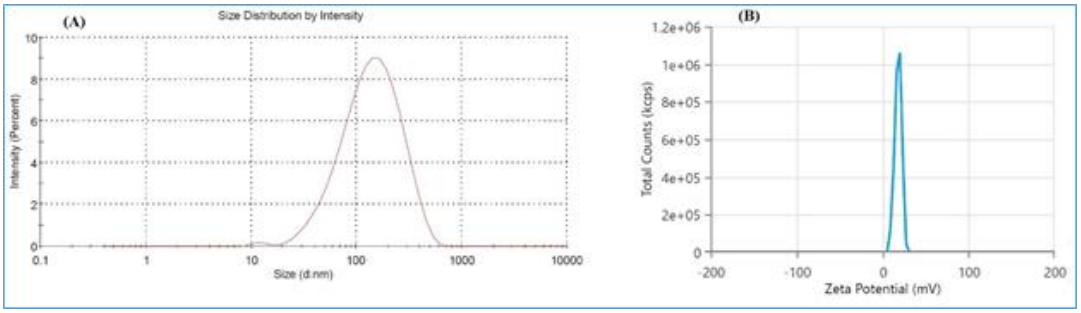

Fig. 1: Particle size and zeta potential of DSN loaded NGs formulation.

The best kinetic model was selected based on the correlation coefficient (R^2) value being closer to 1 (Mujtaba, 2022).

Stability studies

According to ICH guidelines, the stability investigation was carried out. The formulation of DSN-NGs was studied for stability under stress and at room temperature. In order to assess the *in vitro* stability of NGs, they were divided into two portions, with one held at 25°C/60%RH and the other at 40°C/75%RH. Following storage for 0, 1, and 3 months, stability was evaluated for changes in the droplet size, PDI, ZP, and physical appearance.

STATISTICAL ANALYSIS

The data are shown as Mean ± SD. The raw data were analyzed using one-way ANOVA with Graph Pad InStat demo version (GraphPad Software Inc., La Jolla, CA, USA).

RESULTS

Based on factors such as PS, PDI, and LE, the CH:TPP ratio was optimized and it was found that 1: 1 was the best value. The sonication process is likely connected to the production of nanosized particles in NGs. DLS was used to measure the DSN-NGs formulation's size and surface charge (table 1 and fig. 1). NGs were produced after a sonication process and the nanoparticles had a size range between 100 and 200 nm with positive ZP. The prepared gel has been appropriately referred to as NGs because the mean PS of the NGs was approximately 113.07±12.62nm having narrow size distribution (PDI: 0.266) (table 1, fig. 1A).

The ZP of DSN-loaded NGs was 22.32±0.56 mV. (table 1, fig. 1B). The Diosmin-NGs' LE was found to be 81.56±2.65%, whereas the LC was 10.25±1.43%. TEM was used to examine the size and morphology of NGs. Given the deformability of the nanogels and sample preparation, a roughly spherical shape may be assumed based on the microphotographs. The particle size was determined to be between 100 and 200 nm, which is comparable to the findings of the DLS method (fig. 2).

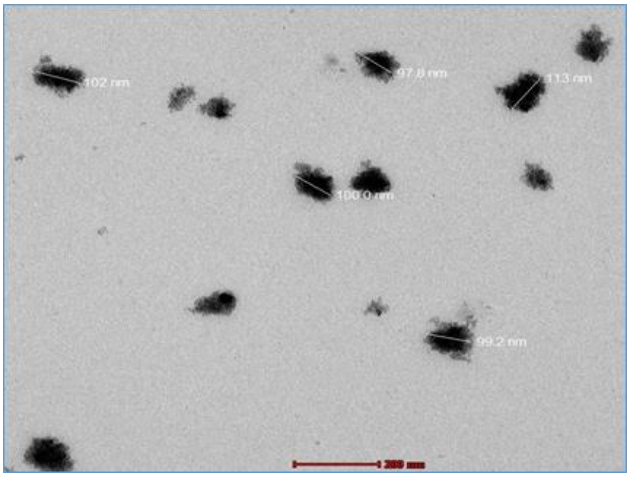

Fig. 2: TEM image of DSN loaded NGs formulation.

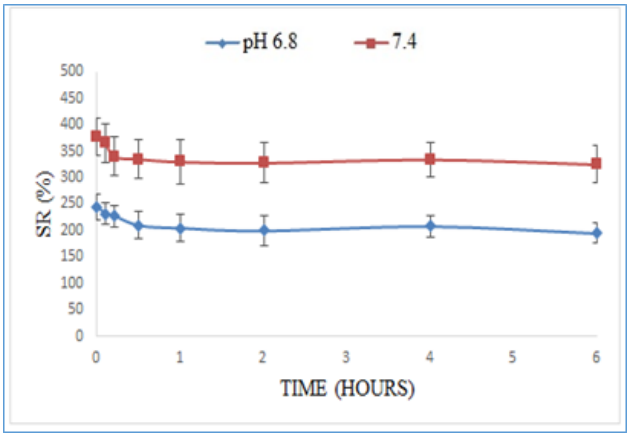

Fig. 3: Swelling behavior of the DSN-NGs formulation in different buffers (pH 6.8 and pH 7.4).

Swelling behaviors

The swelling ratio serves as an indicator of how well NGs can absorb water. Fig. 3 displays the NGs' swelling profiles at pH 6.8 and 7.4 within 30 minutes, the water content in each sample reached equilibrium and the swelling ratios were respectively 210% at pH 6.8 and 335% at pH 7.4.

In vitro drug release and kinetic studies

In pH 1.2 and pH 4.5, the cumulative release of DSN from NGs was found to be 64% and 57% at 4h, respectively and reached the equilibrium condition at around 12h. Comparatively, less than 10% of DSN was released from the NGs at 12 hours in buffers pH 6.8, which was likely caused by the absence of erosion in this media (Yao *et al*., 2016).

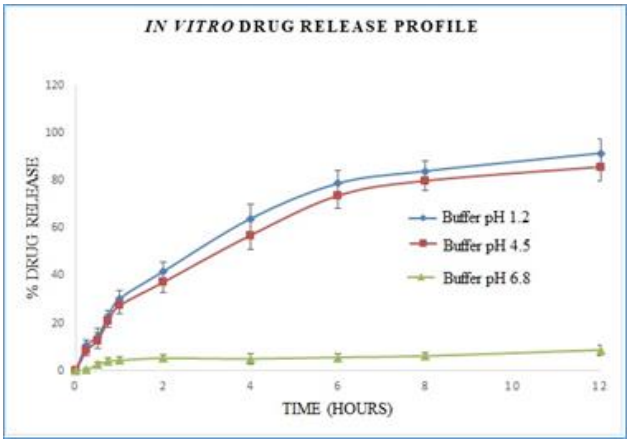

Fig. 4: *In vitro* release profiles of DSN-NGs formulation

Table 2 displays the first-order and korsmeyer-peppas models with R^2 values of 0.9863 and 0.9759, respectively, better representing the release mechanism for DSN-NGs formulation in pH 1.2 acidic buffers. DSN-NGs released by the same mechanism in pH 4.5 acidic buffers as they did in pH 1.2 acidic buffers.

STABILITY STUDIES

According to ICH guidelines, a three-month accelerated stability study was done on the DSN-NGs formulation. table 3 displays how the storage conditions of 25°C/60% RH and 40°C/75% RH affect the characteristics of NGs. Results revealed no significant variation in selected parameters over 90 days.

DISCUSSIONS

One of the most interesting tasks for formulation scientists is the oral delivery of traditional anticancer medicines like DSN. Charge density, drug LE and LC, drug interactions with the pH of the GI tract and enzymatic flora all play a role in the design of an appropriate carrier system for the oral delivery of therapeutic molecules. A positively charged CH solution and a negatively charged TPP solution were used to produce chitosan-based NGs following a previously described ionotropic gelation process (Manivong *et al*., 2022). It is well known that the negatively charged TPP can produce hydrogel nanoparticles with the polycationic polymer CH by creating intra- and intermolecular electrostatic interactions (Nguyen *et al*., 2017). The polymer is dissolved in an acidic environment to encourage the protonation of the amino groups, which results in the generation of positively charged CH, which is necessary for the reaction to take place. Two acids-acetic acid or citric acid-are the principal ones taken into

consideration for this purpose (Wu *et al*., 2014). Positive-charged CH and negatively-charged TPP interacted electrostatically to produce NGs.

The NGs system's smaller particles are likely a result of the continuous sonification process. The ZP determines the electrostatic barriers that can prevent nanoparticle aggregation and agglomeration as a measure of a dispersion system's physical stability (Rachmawati *et al.*, 2013). Additionally, positively charged particles are extremely effective in penetrating and internalizing cell membranes (Liu *et al*., 2018).

Within the polymer network, the NGs were effective at gaining access to and holding onto water molecules, as evidenced by the relatively high swelling ratio, and It is obvious that this capacity was lower in buffers with a pH of 6.8 than it was in buffers with a pH of 7.4. We already know that the hydrophilicity of CH and the types of bonds present within the matrix structure have an impact on the equilibrium water content of NGs. These patterns indicate that a somewhat high pH is favored and that the swelling of CH-based NGs is strongly influenced by the pH (Yao *et al*., 2016).

DSN was released rather quickly during the first two hours, and after that, the cumulative release of DSN increased gradually. This phenomenon was likely caused by the fact that DSN was attached to the surface of the NGs and was quickly released once it came into contact with the release medium, but DSN was still present in the NGs that were released slowly by diffusion due to the gradual erosion or degradation of the DSN-NGs formulation (Yao *et al*., 2016). The sustained release of DSN-NGs prepared by CH may reveal an additional benefit of our formulation as compared to others previously described that showed a burst release (Lotfy *et al*., 2021). The current findings suggest that the DSN release from NGs achieved the equilibrium state with a 90% cumulative release in roughly 12 hours at buffers pH 1.2 and pH 4.5.

The DSN-NGs formulation's *in vitro* release profiles were fitted to mathematical models in order to acquire an understanding of the drug release process. The most efficient model is the one with the highest R^2 values. Therefore, the release mechanism is predicted by the n value of the Korsmeyer-Peppas model; for instance, a value of 0.43 indicates diffusion-controlled (Fickian) release, whereas a value of 0.85 proposes polymer swelling-controlled release. If the polymer swelling and diffusion processes are linked, an anomalous release mechanism would result ($0.43< n <0.85$) (Soni *et al*., 2020). At pH 1.2 and pH 4.5, n had values of 0.26 and 0.27, respectively which suggests a Fickian release mechanism. In conclusion, as demonstrated in the above findings, the erosion feature of NGs with a Fickian mechanism primarily controlled DSN release from NGs, and for the delivery of oral drugs, NGs are considered to be a promising sustained release approach.

CONCLUSION

Our study aimed to establish the use of CH-based nanogels as oral drug delivery platforms for DSN. In this study, the practically insoluble drug DSN was successfully incorporated into CH-NGs prepared by the ionic gelation method which may be a suitable carrier for possible oral delivery. For the oral delivery of DSN, novel CH-based nanogels were prepared and evaluated thoroughly. The optimized NLC exhibited the following properties: droplet size of 113.07nm; polydispersity index of 0.266; zeta potential of 22.32 mV and entrapment efficiency of 81.56% and loading capacity of 10.25%. DSN was released from CH nanogel through the Fickian mechanism in acidic buffers and this release was followed subsequently by swelling and erosion. In summary, CH-based NGs are the potential system for the oral delivery of DSN, and this research widened the scope of NGs' delivery path.

ACKNOWLEDGMENT

The authors gratefully acknowledge the approval and the support of this research study by the grant no. PHAR-2022-11-1512 from the Deanship of Scientific Research at Northern Border University, Arar, KSA.

REFERENCES

Abd El Hady WE, Mohamed EA, Soliman OAE, EL-Sabbagh HM (2019). *In vitro-in vivo* evaluation of chitosan-PLGA nanoparticles for potentiated gastric retention and anti-ulcer activity of diosmin. *Int. J. Nanomedicine*., **14**: 7191-7213

Caristi C, Bellocco E, Panzera V, Toscano G, Vadalà R and Leuzzi U (2003). Flavonoids detection by HPLC-DAD-MS-MS in lemon juices from Sicilian cultivars. *J. Agric. Food Chem.*, **51**(12): 3528-3534.

Di Perri T and Auteri A (1988). Action of S 5682 on the complement system. *In vitro* and *in vivo* study. *Int. Angiol.*, **7**(2): 11-15.

Dung TD, Day CH, Binh TV, Lin CH, Hsu HH, Su CC, Lin YM, Tsai FJ, Kuo WW, Chen LM and Huang CY (2012). PP2A mediates diosmin p53 activation to block HA22T cell proliferation and tumor growth in xenografted nude mice through PI3K-Akt-MDM2 signaling suppression. *Food Chem. Toxicol.,* **50**(5): 1802-1810.

El-Shafae AM and El-Domiaty MM (2001). Improved LC methods for the determination of diosmin and/or hesperidin in plant extracts and pharmaceutical formulations. *J. Pharm. Biomed. Anal*., **26**(4): 539-545.

Havsteen BH (2002). The biochemistry and medical significance of the flavonoids. *Pharmacol Ther*., **96**(2-3): 67-202.

Izzo AA, Carlo GD, Mascolo N, Capasso F and Autore G (1994). Antiulcer effect of flavonoids. Role of endogenous PAF. *Phytother. Res.,* **8**: 179-181.

Kabanov AV and Vinogradov SV (2008). Nanogels as pharmaceutical carriers. In: Torchilin, V. (eds) Multifunctional Pharmaceutical Nanocarriers. Fundamental Biomedical Technologies, vol 4. Springer, New York, NY. pp. 67-80.

Kandaswami C and Middleton E (1994). Free radical scavenging and antioxidant activity of plant flavonoids. *Adv. Exp. Med. Biol.,* **366**: 351-376.

Kurdtabar M, Koutenaee RN and Bardajee GR (2018). Synthesis and characterization of a novel pH-responsive nanocomposite hydrogel based on chitosan for targeted drug release. *J. Polym. Res.,* **25**: 119.

Liu Y, Zheng D, Ma Y, Dai J, Li C, Xiao S, Liu K, Liu J, Wang L, Lei J and He J (2018). Self-Assembled nanoparticles platform based on pectin-dihydroartemisinin conjugates for codelivery of anticancer drugs. *ACS Biomater Sci. Eng.,* **4**(5): 1641-1650.

Lonchampt M, Guardiola B, Sicot N, Bertrand M, Perdrix L and Duhault J (1989). Protective effect of a purified flavonoid fraction against reactive oxygen radicals. *In vivo* and *in vitro* study. *Arzneimittelforschung*. **39**(8): 882-885.

Lotfy NS, Borg TM and Mohamed EA (2021). The promising role of chitosan-poloxamer 188 nanocrystals in improving diosmin dissolution and therapeutic efficacy against ferrous sulfate-induced hepatic injury in rats. *Pharmaceutics*., **13**(12): 2087.

Manivong S, Garcia Ac A, Patten SA, Fernandes JC, Benderdour M, Banquy X, Moldovan F, Roullin VG (2022). Chitosan-Based Nanogels: Synthesis and Toxicity Profile for Drug Delivery to Articular Joints. *Nanomaterials (Basel).* **12**(8): 1337.

Moya-Ortega MD, Alvarez-Lorenzo C, Concheiro A, Loftsson T (2012). Cyclodextrin based nanogels for pharmaceutical and biomedical applications. *Int. J. Pharm.,* **428**: 152-163.

Mujtaba MA (2022). Development of apigenin-loaded niosomes using ecological probe sonication technique for enhanced oral delivery: Application of box-behnken design. *Curr. Pharm. Biotechnol.,* **23**(6): 882-893.

Mujtaba MA, Alotaibi NM, Alshehri SM, Yusuf M, Anwer MK, Rahman MA, Parveen A (2022). Novel therapeutic approach in PEGylated chitosan nanoparticles of apigenin for the treatment of cancer via oral nanomedicine. *Polymers*., **14**(20): 4344.

Nguyen TV, Nguyen TTH, Wang SL, Vo TPK, Nguyen AD (2017). Preparation of chitosan nanoparticles by tpp ionic gelation combined with spray drying and the antibacterial activity of chitosan nanoparticles and a chitosan nanoparticle-amoxicillin complex. *Res. Chem. Intermed.,* **43**: 3527-3537.

Pari L and Srinivasan S (2010). Antihyperglycemic effect of diosmin on hepatic key enzymes of carbohydrate metabolism in streptozotocin-nicotinamide-induced diabetic rats. *Biomed. Pharmacother*., **64**(7): 477-481.

Pérez E, Martínez A, Teijon C, Teijón JM, Blanco MD (2014). Bioresponsive nanohydrogels based on HEAA and NIPA for poorly soluble drugs delivery. *Int. J. Pharm.* **470**: 107-119.

Rachmawati H, Al Shaal L, Müller RH, Keck CM (2013). Development of curcumin nanocrystal: Physical aspects. *J. Pharm. Sci.,* **102**(1): 204-214.

Serra H, Mendes T, Bronze MR, Simplício AL (2008). Prediction of intestinal absorption and metabolism of pharmacologically active flavones and flavanones. *Bioorg. Med. Chem*., **16**(7): 4009-4018.

Sharma S, Kumar A, Deepak, Kumar R, Rana NK, Koch B (2018). Development of a novel chitosan based biocompatible and self-healing hydrogel for controlled release of hydrophilic drug. *Int. J. Biol. Macromol.,* **116**: 37-44.

Soni K, Mujtaba A, Akhter MH and Kohli K (2020). The development of pemetrexed diacid-loaded gelatin-cloisite 30b (mmt) nanocomposite for improved oral efficacy against cancer: Characterization, *in-vitro* and *ex-vivo* assessment. *Curr. Drug Deliv.* **17**(3): 246-256.

Soni K, Mujtaba A, Akhter MH, Zafar A, Kohli K (2020). Optimisation of ethosomal nanogel for topical nano-CUR and sulphoraphane delivery in effective skin cancer therapy. *J. Microencapsul.,* **37**(2): 91-108.

Wu QX, Lin DQ and Yao SJ (2014). Design of chitosan and its water soluble derivatives-based drug carriers with polyelectrolyte complexes. *Mar. Drugs*, **12**(12): 6236-6253.

Yao Y, Xia M, Wang H, Li G, Shen H, Ji G, Meng Q, Xie Y (2016). Preparation and evaluation of chitosan-based nanogels/gels for oral delivery of myricetin. *Eur J Pharm Sci.,* **91**: 144-153.

Yu S, Zhang X, Tan G, Tian L, Liu D, Liu Y, Yang X, Pan W (2017). A novel pH-induced thermosensitive hydrogel composed of carboxymethyl chitosan and poloxamer cross-linked by glutaraldehyde for ophthalmic drug delivery. *Carbohydr. Polym.,* **155**: 208-217.